ENHANCED TURBO MMSE EQUALIZATION FOR MIMO-OFDM OVER RAPIDLY TIME-VARYING FREQUENCY-SELECTIVE CHANNELS

Luca Rugini[1], *Paolo Banelli*[1], *Kun Fang*[2], *and Geert Leus*[2]

[1] DIEI, University of Perugia, Via G. Duranti 93, 06125 Perugia, Italy
[2] Delft University of Technology, Dept. Electrical Eng., 2628 CD Delft, The Netherlands

ABSTRACT

We present iterative turbo-like equalizers for multiple-input multiple-output (MIMO) orthogonal frequency-division multiplexing (OFDM) systems subject to frequency-selective channels with rapid time variation. The proposed equalizers are obtained from a Bayesian approach based on the unbiased minimum mean-squared error (MMSE) criterion, but also admit a probabilistic data association (PDA) interpretation. Two equalizers are discussed: a basic version that makes use of symbol-level variance estimation, and an enhanced version that takes advantage of bit-level variance estimation. Simulation results show that both the presented equalizers outperform a previously proposed MMSE decision-feedback equalizer (DFE) of comparable complexity.

Index Terms— Iterative (turbo) equalization, MIMO-OFDM, time-varying frequency-selective channels

1. INTRODUCTION

Wireless communications based on multiple antennas have initially gained popularity due to the capacity increase in flat-fading channels [1]. In frequency-selective channels, this feature can be maintained by enabling OFDM, so that each subcarrier experiences a separate flat-fading MIMO channel. Notably, in frequency-selective channels, spatial multiplexing MIMO-OFDM is able to offer both a rate increase and a diversity gain with respect to single-antenna OFDM [2]. However, it is expected that future wireless communications will adopt higher carrier frequencies, thereby increasing the Doppler effect caused by relative motion between transmitter and receiver. Since the intercarrier interference (ICI) generated by rapidly time-varying channels destroys the OFDM orthogonality, nontrivial equalization is required (see [3][4] and references therein). In MIMO-OFDM systems, unfortunately, the amount of ICI increases, because of multiple transmit antennas [5]. As a result, ICI mitigation is even more necessary in this scenario.

Among the ICI mitigation techniques for MIMO-OFDM, one of the first proposals is the block linear equalizer (BLE) of [5], which is equivalent to linear MMSE equalization. However, the computational complexity is cubic in the number of subcarriers. To reduce complexity with negligible performance loss, a receiver window matched to the channel Doppler spectrum can be included. This way, the ICI support is reduced, and the frequency-domain (FD) channel matrix can be regarded as banded, leading to linear complexity in the number of subcarriers [6]. More advanced MIMO-OFDM equalizers exploit hard-decision-based ICI cancellation, such as the banded MMSE decision-feedback equalizer (DFE) [6], the V-BLAST-based successive ICI canceller [7], and the parallel ICI canceller with combining [8]. Iterative soft-ICI cancellers can improve performance, such as in [9], which however neglects the ICI at the first step.

In this paper, we present a block turbo equalizer (BTE) based on the banded MMSE-BLE approach [6], in such a way to keep linear complexity. Iterative or turbo equalizers are widely employed in many communication systems, such as code-division multiple-access (CDMA) [10][11], single-carrier [12]-[14], MIMO [15], and OFDM [3][16]. Therefore, different algorithms originally developed in other contexts could be tailored to the MIMO-OFDM scenario. Specifically, we suggest an unbiased MMSE-BTE that exploits the reliability of the data symbols estimated at the previous iteration. Moreover, we propose an enhanced MMSE-BTE that takes advantage of bit-level reliability. Simulation results show that both the proposed equalizers outperform the banded DFE of [6], and can be used even in the presence of more transmit than receive antennas.

Throughout the paper, for simplicity we assume that the equalizers are aware of the MIMO channel. In practice, the channel has to be estimated, e.g., by using the techniques in [7][17][18]. We also assume that the channel Doppler spectrum is known to the receiver, as well as perfect frequency and time synchronization.

2. MIMO-OFDM SYSTEM MODEL

A transmission scheme with M_{T} transmit antennas, M_{R} receive antennas, and N subcarriers is considered. We assume that the $M_{\mathrm{T}}M_{\mathrm{R}}$ multiple channels are both frequency- and time-selective, and share the same second-order statistics. This assumption is realistic because the antennas of the mobile transmitter (receiver) are co-located. The maximum delay spread is assumed lower than the cyclic prefix (CP) length L. At the jth receive antenna, the received vector, after FFT and CP elimination, is expressed by [5]

$$\underline{\mathbf{z}}_j = \sum_{i=1}^{M_{\mathrm{T}}} \underline{\mathbf{\Lambda}}_{j,i}\, \underline{\mathbf{a}}_i + \underline{\mathbf{n}}_j \,, \qquad (1)$$

where $\underline{\mathbf{z}}_j$ is the received vector with size N, $\underline{\mathbf{\Lambda}}_{j,i}$ is the $N \times N$ FD channel matrix that links the ith transmit antenna to the jth receive antenna, $\underline{\mathbf{a}}_i$ is the OFDM data block of size N transmitted by the ith antenna, and $\underline{\mathbf{n}}_j$ is the noise vector at the jth receive antenna. We assume that the transmitted data are i.i.d. QPSK symbols with mapping $a = (1-2c_{\mathrm{I}} + j(1-2c_{\mathrm{Q}}))/\sqrt{2}$, where c_{I} (c_{Q}) is the corresponding bit in the in-phase (quadrature) component. Anyway, the algorithms proposed in this paper can be straightforwardly extended to other constellations.

Each FD channel matrix can be expressed as $\underline{\mathbf{\Lambda}}_{j,i} = \mathbf{F}\mathbf{\Delta}\underline{\mathbf{H}}_{j,i}\mathbf{F}^{H}$, where $\underline{\mathbf{H}}_{j,i}$ is the corresponding $N \times N$ time-domain (TD) channel matrix, $\mathbf{F}$ is the $N \times N$ unitary FFT matrix, and $\mathbf{\Delta} = \mathrm{diag}(\mathbf{w})$, where $\mathbf{w}$ is a TD receiver window of length N; in conventional

OFDM systems, where windowing is absent, $\mathbf{\Delta} = \mathbf{I}_N$. In the presence of Doppler spread, the FD channel matrix $\underline{\mathbf{\Lambda}}_{j,i}$ is no longer diagonal, due to the ICI. However, a properly designed window $\mathbf{w}$ reduces the ICI support, making $\underline{\mathbf{\Lambda}}_{j,i}$ "more" banded [3]. This operation highly reduces the ICI error model of low-complexity banded equalizers, i.e., those equalizers that counteract only the main band of the FD channel matrix [4]. The noise term is expressed as $\underline{\mathbf{n}}_j = \mathbf{F}\underline{\mathbf{\Delta}}\underline{\mathbf{v}}_j$, where $\underline{\mathbf{v}}_j$ is the TD complex additive white Gaussian noise (AWGN) vector at the *j*th receive antenna, with zero mean and covariance $E\{\underline{\mathbf{v}}_j \underline{\mathbf{v}}_j^H\} = \sigma_v^2 \mathbf{I}_N$.

By assuming N_A active subcarriers, the data vector $\underline{\mathbf{a}}_i$ transmitted by the *i*th antenna is rewritten as $\underline{\mathbf{a}}_i = \mathbf{T}_\mathrm{GB}\mathbf{a}_i$, where $\mathbf{a}_i$ is the useful data vector of size N_A, and $\mathbf{T}_\mathrm{GB} = [\mathbf{0}^T_{N_\mathrm{V}/2\times N_\mathrm{A}} \ \mathbf{I}_{N_\mathrm{A}} \ \mathbf{0}^T_{N_\mathrm{V}/2\times N_\mathrm{A}}]^T$ is the $N \times N_\mathrm{A}$ matrix that inserts the $N_\mathrm{V} = N - N_\mathrm{A}$ frequency guard bands. At the receiver, we eliminate the guard bands by $\mathbf{z}_j = \mathbf{R}_\mathrm{GB}\underline{\mathbf{z}}_j$, where $\mathbf{R}_\mathrm{GB} = \mathbf{T}^T_\mathrm{GB}$. By collecting all the received vectors in a unique vector $\mathbf{z} = [\mathbf{z}_1^T \ \cdots \ \mathbf{z}_{M_\mathrm{R}}^T]^T$, we write

$$\mathbf{z} = \mathbf{\Lambda}\,\mathbf{a} + \mathbf{n}\,, \tag{2}$$

with $\mathbf{a} = [\mathbf{a}_1^T \cdots \mathbf{a}_{M_\mathrm{T}}^T]^T$, $\mathbf{\Lambda} = \begin{bmatrix} \mathbf{\Lambda}_{1,1} & \cdots & \mathbf{\Lambda}_{1,M_\mathrm{T}} \\ \vdots & & \vdots \\ \mathbf{\Lambda}_{M_\mathrm{R},1} & \cdots & \mathbf{\Lambda}_{M_\mathrm{R},M_\mathrm{T}} \end{bmatrix}$, $\mathbf{\Lambda}_{i,j} = \mathbf{R}_\mathrm{GB}\underline{\mathbf{\Lambda}}_{i,j}\mathbf{T}_\mathrm{GB}$, and $\mathbf{n} = [\mathbf{n}_1^T \cdots \mathbf{n}_{M_\mathrm{R}}^T]^T$, with $\mathbf{n}_j = \mathbf{R}_\mathrm{GB}\underline{\mathbf{n}}_j$. The noise covariance is $\mathbf{C}_{\mathbf{nn}} = \mathbf{I}_{M_\mathrm{R}} \otimes (\sigma_v^2 \mathbf{W}\mathbf{W}^H)$, where $\mathbf{W} = \mathbf{R}_\mathrm{GB}\mathbf{F}\mathbf{\Delta}$ and $\otimes$ denotes the Kronecker product. We observe that, in (2), adjacent symbols (and adjacent observations) are related to the same antenna and to different subcarriers. Instead, in block-banded designs, adjacent symbols should be related to the same subcarrier and to different antennas. To this end, we define a suitable $MN \times MN$ permutation matrix $\mathbf{P}_{(M,N)}$, with 1's in the positions $\{(i+1, \ \lfloor i/M \rfloor + 1 + N i_{\mathrm{mod}\,M})\}_{i=0}^{MN-1}$ and 0's elsewhere, and rewrite (2) as

$$\boldsymbol{z} = \mathbf{P}_{(M_\mathrm{R},N_\mathrm{A})}\mathbf{z} = \boldsymbol{\Lambda}\boldsymbol{a} + \boldsymbol{n}\,, \tag{3}$$

where $\boldsymbol{\Lambda} = \mathbf{P}_{(M_\mathrm{R},N_\mathrm{A})}\mathbf{\Lambda}\mathbf{P}^T_{(M_\mathrm{T},N_\mathrm{A})}$, $\boldsymbol{a} = \mathbf{P}_{(M_\mathrm{T},N_\mathrm{A})}\mathbf{a}$, and $\boldsymbol{n} = \mathbf{P}_{(M_\mathrm{R},N_\mathrm{A})}\mathbf{n}$. This way, the MIMO-OFDM channel matrix $\boldsymbol{\Lambda}$ in (3) is approximately block-banded. As a consequence, we neglect the ICI coming from faraway subcarriers, and we replace the exact $\boldsymbol{\Lambda}$ with its block-banded approximation $\boldsymbol{B}_{(Q)}$, as expressed by

$$\boldsymbol{B}_{(Q)} = \boldsymbol{\Lambda} \circ \boldsymbol{\Theta}_{(Q)}\,, \tag{4}$$

where $\circ$ denotes the Hadamard product, $\boldsymbol{\Theta}_{(Q)} = \mathbf{\Theta}_{(Q)} \otimes \mathbf{1}_{M_\mathrm{R}\times M_\mathrm{T}}$, and $\mathbf{\Theta}_{(Q)}$ is the $N_\mathrm{A} \times N_\mathrm{A}$ Toeplitz matrix defined as $[\mathbf{\Theta}_{(Q)}]_{m,n} = 1$ for $|m-n| \le Q$ and $[\mathbf{\Theta}_{(Q)}]_{m,n} = 0$ for $|m-n| > Q$. Since the design parameter Q controls the width of the matrix band, it is used to trade off performance for complexity. Using (4), Eq. (3) can be rewritten as

$$\boldsymbol{z} = \boldsymbol{B}_{(Q)}\boldsymbol{a} + \boldsymbol{E}_{(Q)}\boldsymbol{a} + \boldsymbol{n} \approx \boldsymbol{B}_{(Q)}\boldsymbol{a} + \boldsymbol{n}\,, \tag{5}$$

where the out-of-band ICI term $\boldsymbol{E}_{(Q)} = \boldsymbol{\Lambda} - \boldsymbol{B}_{(Q)}$ is neglected. Since $\boldsymbol{B}_{(Q)}$ is block-banded, the right-hand side of (5) enables the design of low-complexity banded equalizers [4][6].

3. BLOCK TURBO MMSE EQUALIZATION

Block equalizers like [6][10][14] jointly estimate all the symbols in a given block, whereas sequential or serial equalizers separately estimate each data symbol [3][12][13]. Although block equalizers are in general more complex, the block-banded structure of $\boldsymbol{B}_{(Q)}$ permits a remarkable complexity reduction, with little performance loss. The equalizers considered herein follow the block approach.

3.1. Banded MMSE Block Turbo Equalizer

Since the banded MMSE-BLE of [6] produces fairly good symbol estimates, these estimates can be exploited to iteratively refine the equalization in a turbo fashion. This idea has been proven to effectively counteract the ICI in single-antenna OFDM systems [16]. We apply a similar approach for MIMO-OFDM, in order to jointly compensate for the ICI caused by Doppler spreading and for the multiple-antenna interference due to spatial multiplexing.

Let us indicate the iteration index with the superscript *k*. We define $\boldsymbol{m}^{(k)} = E\{\boldsymbol{a}\}$ as the prior knowledge about the symbols to be estimated, and $\boldsymbol{V}^{(k)} = E\{(\boldsymbol{a} - \boldsymbol{m}^{(k)})(\boldsymbol{a} - \boldsymbol{m}^{(k)})^H\}$ as the prior knowledge about their covariance, at iteration *k*. By the knowledge of $\boldsymbol{m}^{(k)}$ and $\boldsymbol{V}^{(k)}$, a Bayesian MMSE approach leads to [19]

$$\tilde{\boldsymbol{a}}^{(k)} = \boldsymbol{V}^{(k)}\boldsymbol{B}^H_{(Q)}(\boldsymbol{B}_{(Q)}\boldsymbol{V}^{(k)}\boldsymbol{B}^H_{(Q)} + \mathbf{C}_{\boldsymbol{nn}})^{-1}(\boldsymbol{z} - \boldsymbol{B}_{(Q)}\boldsymbol{m}^{(k)}) + \boldsymbol{m}^{(k)}\,, \tag{6}$$

where $\tilde{\boldsymbol{a}}^{(k)}$ represents the soft estimate of the symbol vector with size $M_\mathrm{T}N_\mathrm{A}$, and $\mathbf{C}_{\boldsymbol{nn}} = (\sigma_v^2 \mathbf{W}\mathbf{W}^H) \otimes \mathbf{I}_{M_\mathrm{R}}$. Although we assume QPSK, we slightly modify (6) to obtain unbiased estimates, in such a way that the same equalizer expression can be used for QAM without scaling the decision thresholds. This leads to

$$\tilde{\boldsymbol{a}}^{(k)} = (\boldsymbol{T}^{(k)})^{-1}\boldsymbol{B}^H_{(Q)}(\boldsymbol{B}_{(Q)}\boldsymbol{V}^{(k)}\boldsymbol{B}^H_{(Q)} + \mathbf{C}_{\boldsymbol{nn}})^{-1}(\boldsymbol{z} - \boldsymbol{B}_{(Q)}\boldsymbol{m}^{(k)}) + \boldsymbol{m}^{(k)}\,, \tag{7}$$

where $\boldsymbol{T}^{(k)}$ is an $M_\mathrm{T}N_\mathrm{A} \times M_\mathrm{T}N_\mathrm{A}$ diagonal matrix that contains the multiplicative effect of the bias at iteration *k*, expressed by

$$\boldsymbol{T}^{(k)} = \left(\boldsymbol{B}^H_{(Q)}(\boldsymbol{B}_{(Q)}\boldsymbol{V}^{(k)}\boldsymbol{B}^H_{(Q)} + \mathbf{C}_{\boldsymbol{nn}})^{-1}\boldsymbol{B}_{(Q)}\right) \circ \mathbf{I}_{M_\mathrm{T}N_\mathrm{A}}\,. \tag{8}$$

At the beginning, we set $k = 1$. Since there is no prior knowledge, $\boldsymbol{m}^{(1)} = \mathbf{0}_{M_\mathrm{T}N_\mathrm{A}\times 1}$ and $\boldsymbol{V}^{(1)} = \mathbf{I}_{M_\mathrm{T}N_\mathrm{A}\times M_\mathrm{T}N_\mathrm{A}}$. Hence, (6) coincides with the biased MMSE-BLE [6] $\tilde{\boldsymbol{a}}^{(1)} = \boldsymbol{B}^H_{(Q)}(\boldsymbol{B}_{(Q)}\boldsymbol{B}^H_{(Q)} + \mathbf{C}_{\boldsymbol{nn}})^{-1}\boldsymbol{z}$, while (7) reduces to its unbiased modification. But after the first iteration, the estimated vector $\tilde{\boldsymbol{a}}^{(k)}$ contains useful information about the transmitted bits. To quantify this information, we define the *a priori* log-likelihood ratio (LLR) and the *a posteriori* LLR as [12]

$$\lambda_\mathrm{pri}(c_{l,\mathrm{I}}) = \ln\frac{\Pr\{c_{l,\mathrm{I}} = 0\}}{\Pr\{c_{l,\mathrm{I}} = 1\}}\,, \quad \lambda_\mathrm{post}(c_{l,\mathrm{I}}) = \ln\frac{\Pr\{c_{l,\mathrm{I}} = 0 \,|\, \tilde{a}^{(k)}_{l,\mathrm{I}}\}}{\Pr\{c_{l,\mathrm{I}} = 1 \,|\, \tilde{a}^{(k)}_{l,\mathrm{I}}\}}\,, \tag{9}$$

respectively, where $c_{l,\mathrm{I}}$ represents the *l*th in-phase bit of $\boldsymbol{a}$, and $\tilde{a}^{(k)}_{l,\mathrm{I}}$ is the *l*th estimated symbol in $\mathrm{Re}\{\tilde{\boldsymbol{a}}^{(k)}\}$ (similar expressions hold true for the quadrature bit $c_{l,\mathrm{Q}}$). We also define the extrinsic LLR as

$$\lambda_\mathrm{extr}(c_{l,\mathrm{I}}) = \lambda_\mathrm{post}(c_{l,\mathrm{I}}) - \lambda_\mathrm{pri}(c_{l,\mathrm{I}})\,, \tag{10}$$

which represents the amount of additional information on the bit $c_{l,\mathrm{I}}$ gained by the equalizer. By assuming a Gaussian probability density function (pdf) $p(\tilde{a}^{(k)}_l \,|\, a_l = \alpha)$, where $a_l = a_{l,\mathrm{I}} + j a_{l,\mathrm{Q}}$ and $\alpha \in \{(\pm 1 \pm j)/\sqrt{2}\}$ is one of the four QPSK points, and approximating $\boldsymbol{V}^{(k)}$ as diagonal, it can be shown that (7) leads to [16]

$$\begin{aligned} \boldsymbol{\lambda}^{(k)}_{\mathrm{extr,I}} &= \sqrt{8}\,((\boldsymbol{T}^{(k)})^{-1} - \boldsymbol{V}^{(k)})^{-1}\,\mathrm{Re}\{\tilde{\boldsymbol{a}}^{(k)}\}\,, \\ \boldsymbol{\lambda}^{(k)}_{\mathrm{extr,Q}} &= \sqrt{8}\,((\boldsymbol{T}^{(k)})^{-1} - \boldsymbol{V}^{(k)})^{-1}\,\mathrm{Im}\{\tilde{\boldsymbol{a}}^{(k)}\}\,, \end{aligned} \tag{11}$$

where $\boldsymbol{\lambda}^{(k)}_{\mathrm{extr,I}} = [\lambda_\mathrm{extr}(c_{1,\mathrm{I}}) \cdots \lambda_\mathrm{extr}(c_{M_\mathrm{T}N_\mathrm{A},\mathrm{I}})]^T$ at iteration *k*, and $\boldsymbol{\lambda}^{(k)}_{\mathrm{extr,Q}}$ is defined in the same way. By similarly defining $\boldsymbol{\lambda}^{(k)}_{\mathrm{pri,I}}$, $\boldsymbol{\lambda}^{(k)}_{\mathrm{pri,Q}}$, $\boldsymbol{\lambda}^{(k)}_{\mathrm{post,I}}$, and $\boldsymbol{\lambda}^{(k)}_{\mathrm{post,Q}}$, the unbiased MMSE-BTE algorithm can be summarized as follows.

Symbol-level MMSE-BTE algorithm

00. Choose the bandwidth parameter Q and the maximum number of iterations K;
01. Set the iteration index $k=1$;
02. If $k=1$, set $\boldsymbol{\lambda}_{\text{pri,I}}^{(1)}=\mathbf{0}_{M_{\text{T}}N_{\text{A}}\times 1}$ and $\boldsymbol{\lambda}_{\text{pri,Q}}^{(1)}=\mathbf{0}_{M_{\text{T}}N_{\text{A}}\times 1}$, otherwise set $\boldsymbol{\lambda}_{\text{pri,I}}^{(k)}=\boldsymbol{\lambda}_{\text{post,I}}^{(k-1)}$ and $\boldsymbol{\lambda}_{\text{pri,Q}}^{(k)}=\boldsymbol{\lambda}_{\text{post,Q}}^{(k-1)}$;
03. Evaluate the a priori symbol mean as [12]

$$\boldsymbol{m}^{(k)}=\frac{\sqrt{2}}{2}\left(\tanh\frac{\boldsymbol{\lambda}_{\text{pri,I}}^{(k)}}{2}+j\tanh\frac{\boldsymbol{\lambda}_{\text{pri,Q}}^{(k)}}{2}\right); \quad (12)$$

04. Evaluate the a priori symbol variance as [12]

$$\boldsymbol{V}^{(k)}=\mathbf{I}_{M_{\text{T}}N_{\text{A}}}-\text{Diag}(\boldsymbol{m}^{(k)})\,\text{Diag}(\boldsymbol{m}^{(k)})^{H}; \quad (13)$$

05. Evaluate $\boldsymbol{T}^{(k)}$ as in (8), using $\boldsymbol{V}^{(k)}$ from (13);
06. Estimate the symbol vector $\tilde{\boldsymbol{a}}^{(k)}$ using (7) with $\boldsymbol{m}^{(k)}$, $\boldsymbol{V}^{(k)}$, and $\boldsymbol{T}^{(k)}$ expressed by (12), (13), and (8), respectively;
07. Evaluate the extrinsic LLR's $\boldsymbol{\lambda}_{\text{extr,I}}^{(k)}$ and $\boldsymbol{\lambda}_{\text{extr,Q}}^{(k)}$ using (11);
08. Evaluate the a posteriori LLR using $\boldsymbol{\lambda}_{\text{post,I}}^{(k)}=\boldsymbol{\lambda}_{\text{pri,I}}^{(k)}+\boldsymbol{\lambda}_{\text{extr,I}}^{(k)}$ and $\boldsymbol{\lambda}_{\text{post,Q}}^{(k)}=\boldsymbol{\lambda}_{\text{pri,Q}}^{(k)}+\boldsymbol{\lambda}_{\text{extr,Q}}^{(k)}$;
09. If $k=K$, terminate the iterative procedure with output $\boldsymbol{\lambda}_{\text{post,I}}^{(K)}$ and $\boldsymbol{\lambda}_{\text{post,Q}}^{(K)}$, otherwise set $k\leftarrow k+1$ and go back to Line 02.

As far as complexity is concerned, most of the operations are spent in Line 06, where the symbol estimation (7) is performed. The major cost of (7) is computing $\boldsymbol{A}_{(Q)}^{(k)}=\boldsymbol{B}_{(Q)}\boldsymbol{V}^{(k)}\boldsymbol{B}_{(Q)}^{H}+\mathbf{C}_{\boldsymbol{nn}}$, which is $O(Q^2M_{\text{T}}M_{\text{R}}^2N_{\text{A}})$ [6], and performing the inverse of $\boldsymbol{A}_{(Q)}^{(k)}$. However, by employing MBAE-SOE windows [4], $\mathbf{C}_{\boldsymbol{nn}}$ is block-banded, and therefore low-complexity algorithms for inverting $\boldsymbol{A}_{(Q)}^{(k)}$ are available [20]. Actually, matrix inversion is circumvented by means of low-complexity routines for block-banded factorizations, which leads to $O(Q^2M_{\text{R}}^3N_{\text{A}})$ [6]. As a result, the computational complexity of the unbiased banded MMSE-BTE is $O(KQ^2\max\{M_{\text{T}},M_{\text{R}}\}M_{\text{R}}^2N_{\text{A}})$ per data block, i.e., linear in the number of subcarriers. Low-complexity algorithms can be employed also for the computation of $\boldsymbol{T}^{(k)}$ in (8), because only the main block-band of $(\boldsymbol{A}_{(Q)}^{(k)})^{-1}$ is necessary [20].

When the symbol constellation is different from QPSK, the presented banded MMSE-BTE algorithm only requires minor modifications. For instance, for 8-PSK, three prior LLR's have to be used, and (12) has to be replaced by a different expression (see Table II in [12]). Anyway, since the unbiased MMSE equalizer (7) stays the same, the computational complexity does not change significantly. This is a key point for multilevel constellations such as 16-QAM, i.e., when unbiased MMSE turbo equalizers outperform biased ones [14]. We also note that, like the serial turbo equalizer in [3], our BTE does not include any channel decoder; anyway, channel decoding (e.g., convolutional) can be easily incorporated into the turbo loop [16].

We now discuss three alternative approaches that lead to the same unbiased MMSE-BTE, which we have presented as an iterative Bayesian linear MMSE equalizer aided by nonlinear soft decisions (12). Specifically, in (7), a unique matrix $\boldsymbol{A}_{(Q)}^{(k)}=\boldsymbol{B}_{(Q)}\boldsymbol{V}^{(k)}\boldsymbol{B}_{(Q)}^{H}+\mathbf{C}_{\boldsymbol{nn}}$ is used for all the subcarriers. On the contrary, the *turbo principle*, when estimating the ith symbol, forces the ith entry of $\boldsymbol{m}^{(k)}$ to zero, and the (i,i)th entry of $\boldsymbol{V}^{(k)}$ to one. However, by the matrix inversion lemma, it can be shown that the (biased) turbo-principle-based approach produces the same estimated vector $\tilde{\boldsymbol{a}}^{(k)}$ of (7), apart from a diagonal bias matrix (see [16] for single-antenna OFDM). Therefore, the turbo-principle-based approach is essentially equivalent to the proposed Bayesian approach. Moreover, a minimum variance unbiased (MVU) BTE has been derived in [14] using *soft interference cancellation*, for single-antenna single-carrier systems subject to time-invariant channels. Despite the different scenario, after few mathematical manipulations, the expression of the MVU-BTE [14] is formally equivalent to the unbiased MMSE-BTE in (7). Hence, also the soft-ICI-cancellation-based approach brings us to the same equalizer obtained by our Bayesian approach. In addition, there also exists an interesting connection with the *probabilistic data association* (PDA) approach, which is equivalent to the (biased) MMSE-BTE with soft interference cancellation [21]. The connection between PDA and turbo MMSE equalizers becomes clear if we consider that both approaches update a posteriori probabilities (or LLR's) using Gaussian approximations. However, the equivalence (proved in [21] for single-carrier MIMO systems) is not straightforward, because turbo MMSE equalizers usually employ scalar Gaussian approximations, whereas PDA exploit vector Gaussian approximations.

The connection between the proposed MMSE-BTE and PDA-based equalizers opens the way to some considerations about the expected performance gain provided by the turbo iterations. Bearing in mind the equivalence with soft ICI cancellation, we expect that the proposed equalizer should outperform hard-decision ICI cancellers, such as DFE [15]. But PDA is generally regarded as a near maximum-likelihood technique, and hence a substantial performance gain is expected. In particular, some PDA methods are applied also in the overloaded case, when the channel matrix is fat [15]. As a consequence, we expect that the proposed unbiased MMSE-BTE can work also when there are more transmit than receive antennas.

3.2. Enhanced Equalization Using Bit-Level Processing

We now introduce a simple but effective variation of the previous unbiased banded MMSE-BTE. Clearly, the size of $\boldsymbol{V}^{(k)}$ in (7) is equal to the number of data symbols, and consequently $\boldsymbol{V}^{(k)}$ models the a priori variance at the symbol level. An improved model can be obtained by differentiating the prior knowledge in the in-phase and quadrature components, i.e., by using two different a priori variances for the two bits of the same QPSK symbol. In this case, for a given symbol, when the in-phase bit is badly estimated and the quadrature bit is well estimated, two different variances are used, instead of their average only. This improved model should lead to a performance gain, as already shown in [13] for single-antenna single-carrier systems in time-invariant channels.

To enable the bit-level banded MMSE-BTE, we switch to the real-based model of (5), and we define $\overline{\boldsymbol{z}}=[\text{Re}\{\boldsymbol{z}^T\},\text{Im}\{\boldsymbol{z}^T\}]^T$, $\overline{\mathbf{a}}=[\text{Re}\{\boldsymbol{a}^T\},\text{Im}\{\boldsymbol{a}^T\}]^T$, $\overline{\mathbf{n}}=[\text{Re}\{\boldsymbol{n}^T\},\text{Im}\{\boldsymbol{n}^T\}]^T$, and

$$\overline{\mathbf{B}}_{(Q)}=\begin{bmatrix}\text{Re}\{\boldsymbol{B}_{(Q)}\} & -\text{Im}\{\boldsymbol{B}_{(Q)}\}\\ \text{Im}\{\boldsymbol{B}_{(Q)}\} & \text{Re}\{\boldsymbol{B}_{(Q)}\}\end{bmatrix}. \quad (14)$$

Similarly to Section 2, we permute the elements in such a way that the real and imaginary components of the same symbol are adjacent, so that we can maintain the block-banded structure, with real blocks of double size with respect to the complex model. Hence, we define $\overline{\boldsymbol{z}}=\mathbf{P}_{(2,M_{\text{R}}N_{\text{A}})}\overline{\boldsymbol{z}}$, $\overline{\boldsymbol{B}}_{(Q)}=\mathbf{P}_{(2,M_{\text{R}}N_{\text{A}})}\overline{\mathbf{B}}_{(Q)}\mathbf{P}_{(2,M_{\text{T}}N_{\text{A}})}^{T}$, $\overline{\boldsymbol{a}}=\mathbf{P}_{(2,M_{\text{T}}N)}\overline{\mathbf{a}}$, and $\overline{\boldsymbol{n}}=\mathbf{P}_{(2,M_{\text{R}}N_{\text{A}})}\overline{\mathbf{n}}$, and apply to the permuted real vector $\overline{\boldsymbol{z}}$ the modified version of (7), as expressed by

$$\tilde{\overline{\boldsymbol{a}}}^{(k)}=(\overline{\boldsymbol{T}}^{(k)})^{-1}\overline{\boldsymbol{B}}_{(Q)}^{T}(\overline{\boldsymbol{B}}_{(Q)}\overline{\boldsymbol{V}}^{(k)}\overline{\boldsymbol{B}}_{(Q)}^{T}+\mathbf{C}_{\overline{\boldsymbol{nn}}})^{-1}(\overline{\boldsymbol{z}}-\overline{\boldsymbol{B}}_{(Q)}\overline{\boldsymbol{m}}^{(k)})+\overline{\boldsymbol{m}}^{(k)}, \quad (15)$$

where $\tilde{\overline{\boldsymbol{a}}}^{(k)}$, $\overline{\boldsymbol{T}}^{(k)}$, $\overline{\boldsymbol{V}}^{(k)}$, $\mathbf{C}_{\overline{\boldsymbol{nn}}}$ and $\overline{\boldsymbol{m}}^{(k)}$ are the real-valued versions

of their corresponding quantities. By defining the real-extended extrinsic LLR vector as $\bar{\boldsymbol{\lambda}}_{\text{extr}}^{(k)} = \mathbf{P}_{(2,M_{\text{T}}N_{\text{A}})}[\boldsymbol{\lambda}_{\text{extr,I}}^{(k)\ T}, \boldsymbol{\lambda}_{\text{extr,Q}}^{(k)\ T}]^T$, and similarly $\bar{\boldsymbol{\lambda}}_{\text{pri}}^{(k)}$ and $\bar{\boldsymbol{\lambda}}_{\text{post}}^{(k)}$, the enhanced banded MMSE-BTE algorithm can be expressed as follows.

Bit-level MMSE-BTE algorithm

00. Choose the parameter Q and the number of iterations K;
01. Set the iteration index $k = 1$;
02. If $k = 1$, set $\bar{\boldsymbol{\lambda}}_{\text{pri}}^{(1)} = \mathbf{0}_{2M_{\text{T}}N_{\text{A}}\times 1}$, otherwise $\bar{\boldsymbol{\lambda}}_{\text{pri}}^{(k)} = \bar{\boldsymbol{\lambda}}_{\text{post}}^{(k-1)}$;
03. Evaluate the a priori bit mean as $\bar{\boldsymbol{m}}^{(k)} = 2^{-1/2}\tanh(\bar{\boldsymbol{\lambda}}_{\text{pri}}^{(k)}/2)$;
04. Evaluate the a priori bit variance as

$$\bar{\boldsymbol{V}}^{(k)} = \frac{1}{2}\mathbf{I}_{2M_{\text{T}}N_{\text{A}}} - \text{Diag}(\bar{\boldsymbol{m}}^{(k)})\,\text{Diag}(\bar{\boldsymbol{m}}^{(k)})^T; \qquad (16)$$

05. Evaluate $\bar{\boldsymbol{T}}^{(k)} = (\bar{\boldsymbol{B}}_{(Q)}^H(\bar{\boldsymbol{B}}_{(Q)}\bar{\boldsymbol{V}}^{(k)}\bar{\boldsymbol{B}}_{(Q)}^T + \mathbf{C}_{\bar{\boldsymbol{m}}\bar{\boldsymbol{m}}})^{-1}\bar{\boldsymbol{B}}_{(Q)}) \circ \mathbf{I}_{2M_{\text{T}}N_{\text{A}}}$;
06. Estimate the vector $\tilde{\bar{\boldsymbol{a}}}^{(k)}$ using (15);
07. Evaluate the extrinsic LLR $\bar{\boldsymbol{\lambda}}_{\text{extr}}^{(k)} = \sqrt{8}((\bar{\boldsymbol{T}}^{(k)})^{-1} - \bar{\boldsymbol{V}}^{(k)})^{-1}\tilde{\bar{\boldsymbol{a}}}^{(k)}$;
08. Evaluate the a posteriori LLR $\bar{\boldsymbol{\lambda}}_{\text{post}}^{(k)} = \bar{\boldsymbol{\lambda}}_{\text{pri}}^{(k)} + \bar{\boldsymbol{\lambda}}_{\text{extr}}^{(k)}$;
09. If $k = K$, terminate the iterative procedure with output $\bar{\boldsymbol{\lambda}}_{\text{post}}^{(K)}$, otherwise set $k \leftarrow k+1$ and go back to Line 02.

With respect to the symbol-level case, the bit-level MMSE-BTE employs matrices of double dimensions. For instance, the number of mathematical operations in (15) increases of a factor of about *eight* with respect to (7). However, in the bit-level algorithm, the single operations are real-valued and hence less costly. Since one complex multiplication is equivalent to *four* real multiplications, the complexity of the bit-level algorithm is roughly doubled with respect to the symbol-level version. In the first iteration, the two versions give the same results, and hence the symbol-level version is preferable.

We observe that the presented bit-level MMSE-BTE algorithm assumes a diagonal $\bar{\boldsymbol{V}}^{(k)}$ (16) and therefore neglects the crosscorrelation between the real and the imaginary parts of the same symbol. Obviously, the crosscorrelation can be incorporated to further improve performance [13]. In this case, $\bar{\boldsymbol{V}}^{(k)}$ becomes block-diagonal with blocks of size two, and therefore it does not destroy the whole block-banded structure. Noteworthy, the real-imaginary approach can also be applied to other constellation formats [13].

Finally, we remind that a similar iterative approach has been explored in the context of multiuser detection [11]. Indeed, the iterative receiver of [11] employs the so-called *widely linear* (WL) processing to counteract the multiuser interference, which is rotationally variant (or improper). Due to the inclusion of conjugate observations, a WL turbo equalizer would be equivalent to our bit-level algorithm.

4. SIMULATION COMPARISON

We consider an MIMO-OFDM system with $N = 128$, $N_{\text{A}} = 96$, and $L = 8$. We assume that the $M_{\text{T}}M_{\text{R}}$ channels are independent. The power-delay profile follows a truncated exponential distribution with sample-normalized rms delay spread $\sigma = 3$. Each channel path is characterized by Rayleigh fading and Jakes' Doppler spectrum. The maximum Doppler spread is 15% of the subcarrier spacing. For all the banded equalizers, MBAE-SOE windowing [4] is assumed. The SNR is normalized with respect to M_{T}.

Fig. 1 shows the BER performance of the symbol-level banded MMSE-BTE after $K = 2$ iterations, compared with the BER of the full MMSE-BLE [5] and of the banded MMSE-BLE [6], when $M_{\text{T}} = 2$ and $M_{\text{R}} = 2$, as a function of the bandwidth parameter Q. For all Q's, the BTE drastically outperforms the corresponding BLE, at a price of double complexity, which scales with KQ^2. Fig. 2 compares the BER of the proposed equalizers, including the enhanced bit-level version, with the BER of the banded block DFE (BDFE) [6]. The banded BDFE [6] has double complexity with respect to the banded BLE, i.e., the same complexity of the symbol-level banded BTE with $K = 2$. The significant gain of BTE with respect to BDFE is evident. The BER can be improved further by using the enhanced bit-level BTE, paying additional complexity.

We now consider the overloaded case, with $M_{\text{T}} = 3$ transmit and $M_{\text{R}} = 2$ receive antennas, in Figs. 3-4. This scenario is quite challenging because in this case linear methods do not work. Fig. 3 displays that a third iteration can help. From Fig. 4, it is noteworthy that also the BDFE does not work properly; on the contrary, both the proposed BTE's are able to reduce the BER up to 10^{-2}, which is a satisfying result for low-complexity estimators of uncoded bits in overloaded MIMO-OFDM scenarios.

5. CONCLUSIONS

We have proposed two low-complexity iterative banded MMSE block equalizers for MIMO-OFDM systems in rapidly time-varying multipath channels. Simulation results have shown that both equalizers outperform a DFE with comparable complexity, and can be applied in scenarios with more transmit than receive antennas. Future work may consider also space-time-coding (STC) OFDM systems, and a BER performance analysis investigation.

6. REFERENCES

[1] G. J. Foschini, "Layered space-time architecture for wireless communication in a fading environment when using multi-element antennas," *Bell Labs Tech. J.*, pp. 41-59, Autumn 1996.

[2] H. Bölcskei, D. Gesbert, and A. J. Paulraj, "On the capacity of OFDM-based spatial multiplexing systems," *IEEE Trans. Commun.*, vol. 50, pp. 225-234, Feb. 2002.

[3] P. Schniter, "Low-complexity equalization of OFDM in doubly selective channels," *IEEE Trans. Signal Process.*, vol. 52, pp. 1002-1011, Apr. 2004.

[4] L. Rugini, P. Banelli, and G. Leus, "Low-complexity banded equalizers for OFDM systems in Doppler spread channels," *EURASIP J. Appl. Signal Process.*, vol. 2006, Article ID 67404, pp. 1-13, 2006.

[5] A. Stamoulis, S. N. Diggavi, and N. Al-Dhahir, "Intercarrier interference in MIMO OFDM," *IEEE Trans. Signal Process.*, vol. 50, pp. 2451-2464, Oct. 2002.

[6] L. Rugini and P. Banelli, "Banded equalizers for MIMO-OFDM in fast time-varying channels," *EUSIPCO 2006*, Florence, Italy, Sept. 2006.

[7] W.-G. Song and J.-T. Lim, "Channel estimation and signal detection for MIMO-OFDM with time varying channels," *IEEE Commun. Lett.*, vol. 10, pp. 540-542, Jul. 2006.

[8] R. Li, Y. Li and B. Vucetic, "Iterative receiver for MIMO-OFDM systems with joint ICI cancellation and channel estimation," in Proc. *IEEE WCNC 2008*, Las Vegas, USA, pp. 7-12, Mar./Apr. 2008.

[9] M. Zhao, Z. Shi, and M. C. Reed, "An iterative receiver with channel estimation for MIMO-OFDM over a time and frequency dispersive fading channel," in Proc. *IEEE GLOBECOM 2007*, Washington, USA, pp. 4155-4159, Nov. 2007.

[10] X. Wang and H. Poor, "Iterative (turbo) soft interference cancellation and decoding for coded CDMA," *IEEE Trans. Commun.*, vol. 47, pp. 1046-1061, Jul. 1999.

[11] A. Lampe, R. Schober, W. Gerstacker, and J. Huber, "A novel iterative multiuser detector for complex modulation schemes," *IEEE J. Sel. Areas Commun.*, vol. 20, pp. 339-350, Feb. 2002.

[12] M. Tüchler, A. C. Singer, and R. Koetter, "Minimum mean squared error equalization using a priori information," *IEEE Trans. Signal Process.*, vol. 50, pp. 673-683, Mar. 2002.

[13] S. Jiang, L. Ping, H. Sun, and C. S. Leung, "Modified LMMSE turbo equalization," *IEEE Commun. Lett.*, vol. 8, pp. 174-176, Mar. 2004.

[14] M. A. Dangl, C. Sgraja, and J. Lindner, "An improved block equalization scheme for uncertain channel estimation," *IEEE Trans. Wireless Commun.*, vol. 6, pp. 146-156, Jan. 2007.

[15] S. Liu and Z. Tian, "Near-optimum soft decision equalization for frequency selective MIMO channels," *IEEE Trans. Signal Process.*, vol. 52, pp. 721-733, Mar. 2004.

[16] K. Fang, L. Rugini, and G. Leus, "Low-complexity block turbo equalization for OFDM systems in time-varying channels," *IEEE Trans. Signal Process.*, vol. 56, pp. 5555-5566, Nov. 2008.

[17] D. Schafhuber, M. Rupp, G. Matz, and F. Hlawatsch, "Adaptive identification and tracking of doubly selective fading channels for wireless MIMO-OFDM systems," in Proc. *IEEE SPAWC 2003*, Rome, Italy, June 2003, pp. 417-421.

[18] J. Gao and H. Liu, "Low-complexity MAP channel estimation for mobile MIMO-OFDM systems," *IEEE Trans. Wireless Commun.*, vol. 7, pp. 774-780, Mar. 2008.

[19] S. M. Kay, *Fundamentals of Statistical Signal Processing: Estimation Theory*, Prentice-Hall, 1993.

[20] A. Asif and J. M. F. Moura, "Block matrices with *l*-block-banded inverse: Inversion algorithms," *IEEE Trans. Signal Process.*, vol. 53, pp. 630-642, Feb. 2005.

[21] F. Cao, J. Li, and J. Yang, "On the relation between PDA and MMSE-ISDIC," *IEEE Signal Process. Lett.*, vol. 14, pp. 597-600, Sept. 2007.

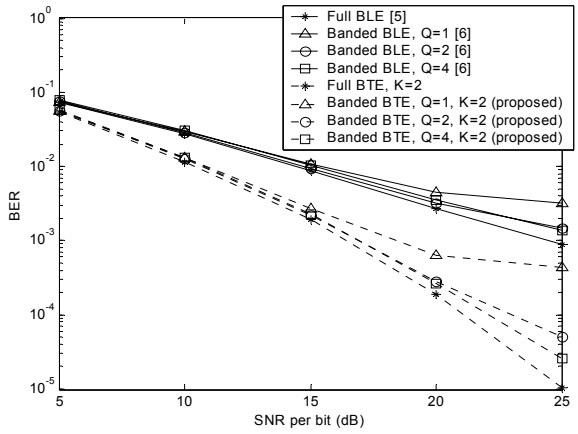

Fig. 1. Effect of the band approximation parameter Q. Same number of transmit and receive antennas, $M_{\mathrm{T}} = M_{\mathrm{R}} = 2$.

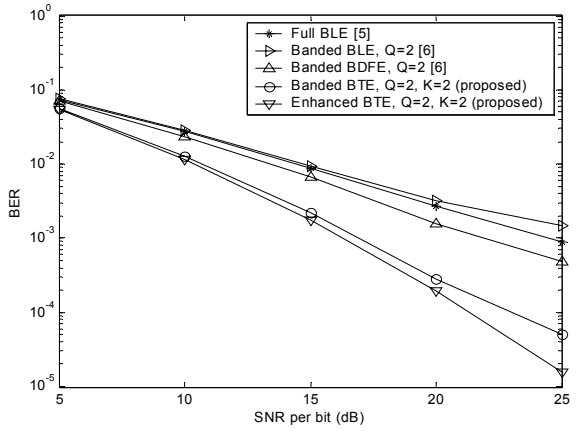

Fig. 2. Performance comparison among various equalizers. Same number of transmit and receive antennas, $M_{\mathrm{T}} = M_{\mathrm{R}} = 2$.

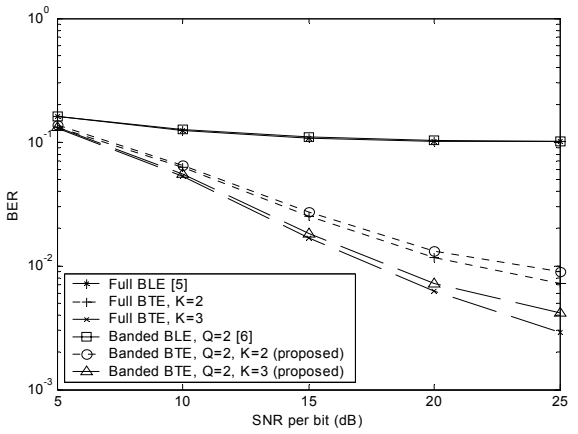

Fig. 3. Effect of the number of iterations K. More transmit than receive antennas (overloaded case), $M_{\mathrm{T}} = 3$, $M_{\mathrm{R}} = 2$.

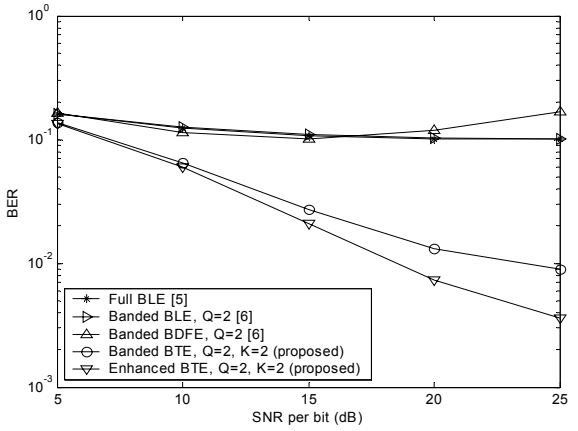

Fig. 4. Performance comparison among various equalizers. More transmit than receive antennas (overloaded case), $M_{\mathrm{T}} = 3$, $M_{\mathrm{R}} = 2$.